TECHNICAL REPORT ARLCB-TR-82007

FRACTURE ANALYSIS OF THICK-WALL CYLINDER PRESSURE VESSELS

J. H. Underwood
D. P. Kendall

April 1982

US ARMY ARMAMENT RESEARCH AND DEVELOPMENT COMMAND
LARGE CALIBER WEAPON SYSTEMS LABORATORY
BENÉT WEAPONS LABORATORY
WATERVLIET, N. Y. 12189

AMCMS No. 61110191A0011

DA Project No. 1L161101A98A

PRON No. 1A2231491A1A

SECURITY CLASSIFICATION OF THIS PAGE *(When Data Entered)*

REPORT DOCUMENTATION PAGE		READ INSTRUCTIONS BEFORE COMPLETING FORM
1. REPORT NUMBER ARLCB-TR-82007	2. GOVT ACCESSION NO. AD-A116 284	3. RECIPIENT'S CATALOG NUMBER
4. TITLE *(and Subtitle)* FRACTURE ANALYSIS OF THICK-WALL CYLINDER PRESSURE VESSELS		5. TYPE OF REPORT & PERIOD COVERED 6. PERFORMING ORG. REPORT NUMBER
7. AUTHOR(s) J. H. Underwood and D. P. Kendall		8. CONTRACT OR GRANT NUMBER(s)
9. PERFORMING ORGANIZATION NAME AND ADDRESS US Army Armament Research & Development Command Benet Weapons Laboratory, DRDAR-LCB-TL Watervliet, NY 12189		10. PROGRAM ELEMENT, PROJECT, TASK AREA & WORK UNIT NUMBERS AMCMS No. 61110191A0011 DA Project No. 1L161101A98 PRON No. 1A2231491A1A
11. CONTROLLING OFFICE NAME AND ADDRESS US Army Armament Research & Development Command Large Caliber Weapon Systems Laboratory Dover, NJ 07801		12. REPORT DATE April 1982 13. NUMBER OF PAGES 40
14. MONITORING AGENCY NAME & ADDRESS*(if different from Controlling Office)*		15. SECURITY CLASS. *(of this report)* UNCLASSIFIED 15a. DECLASSIFICATION/DOWNGRADING SCHEDULE

16. DISTRIBUTION STATEMENT *(of this Report)*

Approved for public release; distribution unlimited.

17. DISTRIBUTION STATEMENT *(of the abstract entered in Block 20, if different from Report)*

18. SUPPLEMENTARY NOTES

Submitted to: Case Studies in Engineering Mechanics and Materials

Presented to: ASTM E-24 Committee on Fracture, Philadelphia, PA, 27-29 April 1982.

19. KEY WORDS *(Continue on reverse side if necessary and identify by block number)*

Fracture Analysis	Residual Stress
Pressure Vessels	Fracture Mechanics
Fatigue Life	Crack Shape

20. ABSTRACT *(Continue on reverse side if necessary and identify by block number)*

Fracture mechanics analysis of cylindrical pressure vessels is described in a brief fracture case study. Also included in this report are additional examples of crack growth in pressure vessels and cannons.

The case study is of an early brittle failure and subsequent redesign of a cannon tube. Fracture mechanics test methods are described which were

(CONT'D ON REVERSE)

DD FORM 1 JAN 73 1473 EDITION OF 1 NOV 65 IS OBSOLETE

UNCLASSIFIED

SECURITY CLASSIFICATION OF THIS PAGE *(When Data Entered)*

20. ABSTRACT (CONT'D)

developed specifically for testing of [illegible]eometries. Three examples of current fracture analysis o[illegible] cylindrical pressure vessels are presented. Fast fracture of a vessel is described, including effects of tension residual stress and crack shape. Evidence of environmentally assisted fracture of a cannon tube is presented. Fatigue crack growth and life calculation methods for cylindrical pressure vessels are developed and checked with experimental results; effects of compressive residual stress due to overstrain are analyzed, including reductions from the expected theoretical residual stress due to reduced compressive strength of the alloy steel.

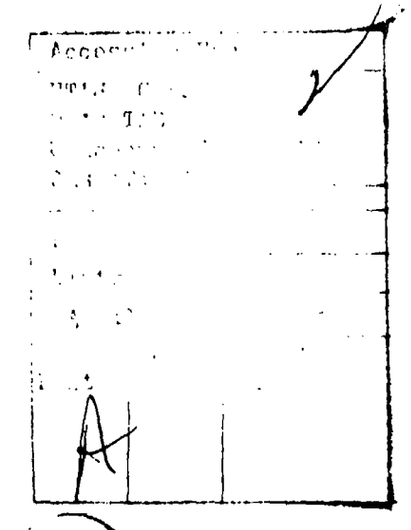

TABLE OF CONTENTS

	Page
ACKNOWLEDGEMENTS	iii
INTRODUCTION	1
AN EARLY FAILURE	1
Failure	1
Redesign	5
TEST METHOD DEVELOPMENT	8
EXAMPLES OF FRACTURE ANALYSIS	10
Fast Fracture	10
Environmental Fracture	13
Fatigue Fracture	15
REFERENCES	22

LIST OF ILLUSTRATIONS

1.	Brittle Failure of 175 mm Cannon Tube.	25
2.	Outline of Failure and Redesign of 175 mm Cannon Tube.	26
3.	Contained Leak-Before-Break Cracking in a Cannon.	27
4.	Circumferential Residual Stress Distributions for Over-strained Cylinders with $r_2/r_1 = 2.0$.	28
5.	Arc Specimens for Fracture Mechanics Tests of Material in Hollow Cylinder Geometries.	29
6.	Stress Intensity Factor, K, Results for Arc Specimen from Experiment and Analysis.	30
7.	Variation of Fracture Toughness with Yield Strength for Ni-Cr-Mo-V Steel Forgings.	31
8.	Fast Fracture Affected by Crack Shape and Tensile Residual Stress.	32

Page

9. Stress Corrosion Cracking in a Cannon Tube. 33

   (a) Location 1 - Mixed Stress Corrosion and Fatigue Cracking; Location 2 - Fast Fracture; Location 3 - Initiation of Stress Corrosion Cracking at Rifling Land; 15X.
   (b) Micrograph of Location 3, 100X.

10. Scanning Electron Microscope Fractographs of Stress Corrosion Initiated Cracking in a Cannon Tube. 34

   (a) Stress Corrosion Cracking at Rifling Land, 400X.
   (b) Fatigue Cracking at Location 1 in Figure 9, 100X.
   (c) Fast Fracture at Location 2 in Figure 9, 1700X.

11. Sketch of Tensile Yielding and Reduced Compressive Yield Strength for 100% Overstrained Steel Cylinder with r_2/r_1 = 2.0. 35

12. Residual Stress and Stress Intensity Factor, K, Distributions for 60% Overstrained Cylinder with r_1 = 2.0, p = 331 MPa, a_i = 6.4 mm, a/2c = 0.5. 36

13. Crack Depth Versus Number of Fatigue Cycles From Experiment and Analysis for Cylinders with 0% and 60% Overstrain, r_1 = 90 mm, r_2/r_1 = 2.0, p = 331 MPa, a_i = 6.4 mm, a/2c = 0.5. 37

ACKNOWLEDGEMENTS

We are pleased to credit Mr. B. B. Brown and co-workers for design and execution of pressure vessel experiments, Mr. F. E. Moscinski and co-workers for metallographic and fractographic analyses, and Mr. J. F. Throop and co-workers for overstrain residual stress experiments.

INTRODUCTION

In basic function a cannon is a pressure vessel, since it must contain pressure in repeated application during its use. Thus, the engineering analysis of fracture of cannons has application to pressure vessels in general. Further, the geometry and materials used for cannons are often used in other pressure vessel applications, such as high pressure piping and high pressure containers for chemical processes. Because of such common features between cannons and other pressure vessels, a description of fracture of cannons should be of relatively general interest.

The objective of this report is to describe some key elements of the fracture analysis of cannon pressure vessels performed by our laboratory, both early and recent work. The discipline of linear elastic fracture mechanics will predominate, because the failure of a cannon is usually a crack growth process. The description is in three parts. First is an outline case study of an early brittle failure of a cannon. This is followed by a summary of recent fracture-test-method development work and finally by examples of fracture analysis, all of which are outgrowths of the early concern with brittle fracture.

AN EARLY FAILURE

Failure

An unexpected failure of a critical structural component is a remarkably effective impetus to engineering analysis. The Army experienced a premature field failure of a cannon tube during the 1960's, and this provided a significant impetus to fracture analysis of cannon, particularly the pressurized com-

ponents. The then new methods of fracture mechanics were used to determine the cause of failure and to help with the redesign in order to prevent any further problems. The details of the failure are described in Reference 1; only certain important features will be discussed here. A photo of the fractured pieces of a component can convey a great deal regarding the nature and extent of the failure. Figure 1 shows the remains of the portion of the 175 mm cannon which was subjected to the highest pressure during firing. The extent of fragmentation in this portion is a clear indication of a classically brittle failure. Some of the fragments were thrown as far as 1000 m, further evidence of brittle fracture. By using fracture mechanics, it should be possible to quantitatively describe this brittle failure and the design changes required to prevent such a failure.

A description of the conditions which led to the brittle failure as well as the redesign conditions is presented in outline form in Figure 2. The basic geometry and the pressure loading, p, of the failure location are given.* See Figure 3 for nomenclature. The material used was a forged alloy steel similar to ASTM A723, Grade 2 for pressure component applications. Conventional air melting practice for the cannon which failed resulted in 7.0 J Charpy impact energy at -40°C and 90 MPa $m^{1/2}$ plane-strain fracture toughness, K_{Ic}, when heat treated to 1180 MPa yield strength, σ_{ys}.

---

[1]Davidson, T. E., Throop, J. F., Underwood, J. H., "Failure of a 175 MM Cannon Tube and the Resolution of the Problem Using an Autofrettage Design," Case Studies in Fracture Mechanics, T. P. Rich and D. J. Cartwright, Eds., AMMRC MS 77-5, Army Materials and Mechanics Research Center, 1977.

*Note that the inner radius of the cylinder, r_1 = 89 mm, is a bit larger than half of the nominal cannon size, because r_1 includes the depth of the rifling grooves.

The critical crack which initiated the failure was found in the area which is subjected to both high pressure and the stress concentrations of the rifling. The deepest fatigue crack in this area became the critical crack with depth, a_c, shape $a_c/2c$, and relative depth, a_c/W as indicated in Figure 2. The critical crack had the C-R* orientation, shown in Figure 3. Fatigue cracks were observed to initiate almost immediately in the cannon; the combination of transformational and thermal stresses at the inner radius during firing could lead to a network of heat-check cracks as deep as 1 mm in about ten firing cycles. Growth from such an initial, heat-check crack to the final depth of 6.4 mm occurred in 600 firing cycles, with most cycles at an internal pressure of 345 MPa. Overlooking for the purposes here the specific processes by which the crack grew, the dominant fact is that brittle fracture occurred with a crack depth of only one tenth of the wall thickness. If it can be shown that the stress intensity factor, K, which was applied to the cannon at failure is close to the measured plane-strain fracture toughness, K_{Ic}, this would explain the failure and initiate a proper approach for redesign.

An expression for K of an internally pressurized cylinder with a C-R orientation surface crack at the inner radius can be written based on a combination of the work of Bowie and Freese[2] and Newman and Raju:[3]

$$K = f_p f_s \, p(\pi a)^{1/2} \qquad (1)$$

---

[2]Bowie, O. L. and Freese, C. E., "Elastic Analysis For a Radial Crack in a Circular Ring," Engineering Fracture Mechanics, Vol. 4, 1972, pp. 315-321.

[3]Newman, J. C., Jr., and Raju, I. S., "An Empirical Stress-Intensity Factor Equation for the Surface Crack," Engineering Fracture Mechanics, Vol. 15, 1981, pp. 185-192.

*Plane normal to the circumferential direction, growth in the radial direction, see ASTM Method E399.

In Equation (1) f_p is a dimensionless factor which accounts for the specific radius ratio, r_2/r_1 and relative crack depth, a/W of the cylinder under consideration; it can be obtained from the collocation results of Reference 2. The factor f_s accounts for the crack shape, a/2c and a/W, and is obtained following some calculations from the equations of Reference 3 which are based on finite element results from plates under tension and bending loads. It is often necessary to use a weighted shape factor, f_s, which accounts for the relative proportions of tension and bending load in a cylinder. For the a/2c and a/W at failure of the cannon here, this is not necessary because f_s for both tension and bending is close to 0.70. This means that K at the point of deepest penetration of the surface crack is 0.70 times that of a straight-fronted crack of the same depth in the cylinder. Using this value and f_p = 2.70 from Reference 2, gives an applied K at failure of 112 MPa $m^{1/2}$, which is 1.24 times the value of K_{Ic}. An applied K required for fracture which is somewhat above K_{Ic} would be expected because of the loss of plane-strain constraint at the crack tip caused by the small crack depth.* Therefore the brittle failure of the cannon is satisfactorily explained, and linear elastic fracture mechanics seems appropriate for use in the redesign process.

---

[2]Bowie, O. L. and Freese, C. E., "Elastic Analysis For a Radial Crack in a Circular Ring," Engineering Fracture Mechanics, Vol. 4, 1972, pp. 315-321.

[3]Newman, J. C., Jr., and Raju, I. S., "An Empirical Stress-Intensity Factor Equation for the Surface Crack," Engineering Fracture Mechanics, Vol. 15, 1981, pp. 185-192.

*When the crack tip is near a free surface, whether due to a shallow crack near the "front" surface or a deep crack near the "back" surface, there is a loss of plane-strain constraint.

Redesign

The objective of the cannon redesign was the same as that often applied to critical pressure vessel components, a leak-before-break criteria for any crack-related failure. When a leak-before-break can be assured, a contained failure of the vessel occurs of the type shown in Figure 3 for a cannon.[4] In this case severe heat-checking of the inner radius (bottom of photo) quickly initiated a crack which grew by fatigue to a point about nine tenths through the wall thickness (light band near top of photo). The final fast failure through to the outer radius occurred as a relatively short, through crack which showed no tendency to run down the axis of the cylinder.

Three basic changes were made with the 175 mm cannon in order to increase the material fracture toughness relative to the applied K and therefore achieve a leak-before-break condition: (1) The specified yield strength was decreased from a nominal 1180 to 1030 MPa. (2) Vacuum melting practice was incorporated for the steel, as is now required in ASTM A723 steel. (3) Compressive residual stresses were produced near the inner radius of the cannon by an overstraining process. The important effect of the first two changes was a significant increase in the average -40°C Charpy impact energy and the fracture toughness, see Figure 2. The primary intended effects of the overstrain residual stress were to compensate for the decrease in yield strength*

---

[4]Underwood, J. H. and Throop, J. F., "Surface Crack K-Estimates and Fatigue Life Calculations in Cannon Tubes," Part-Through Crack Fatigue Life Prediction, ASTM STP 587, J. B. Chang, Ed., American Society for Testing and Materials, 1979, pp. 195-210.

*The compressive residual stress at the inner radius, where the applied tensile stresses are maximum, more than compensates for the drop in tensile yield strength.

and to decrease the rate of growth of fatigue cracks (discussed in an upcoming section). In addition, the residual stress can be seen to have a beneficial effect on brittle fracture.

Expressions are available for the residual stresses in an overstrained cylinder. For the plastically overstrained portion of a cylinder, $r_1 \leq r \leq r_{ys}$, and using the Tresca yield condition, the circumferential residual stress is[5]

$$\frac{\sigma_{\theta-R}}{\sigma_{ys}} = \left[\left(\frac{r_1^2}{r_2^2-r_1^2}\right)\left(1 + \frac{r_2^2}{r^2}\right)\left(\frac{r_{ys}^2-r_2^2}{2r_2^2} - \ln\frac{r_{ys}}{r_1}\right) + \left(\frac{r_{ys}^2+r_2^2}{2r_2^2} - \ln\frac{r_y}{r}\right)\right] \quad (2)$$

For the elastic portion of a partially overstrained cylinder, $r_{ys} \leq r \leq r_2$,[5]

$$\frac{\sigma_{\theta-R}}{\sigma_{ys}} = \left[1 + \frac{r_2^2}{r^2}\right]\left[\frac{r_{ys}^2}{2r_2^2} + \frac{r_1^2}{r_2^2-r_1^2}\left(\frac{r_{ys}^2-r_2^2}{2r_2^2} - \ln\frac{r_{ys}}{r_1}\right)\right] \quad (3)$$

Figure 4 shows plots of Equations (2) and (3) for a cylinder with $r_2/r_1 = 2.0$ for 50% and 100% overstrain conditions, that is, for ideal overpressures of a cylinder where plastic deformation proceeds half and full way through the wall thickness. Also shown in Figure 4 are modified residual stress distributions which are corrected for the reduction in compressive yield strength which occurs in the steel considered here following tensile yielding. For example, following the approximately 1% tensile plastic strain at the inner radius which occurs during 100% overstrain of an $r_2/r_1 = 2.0$ cylinder, the compressive yield strength is only 0.53 times the unaffected value,[6] so the residual

---

[5]Davidson, T. E., Kendall, D. P. and Reiner, A. N., "Residual Stresses in Thick-Walled Cylinders Resulting From Mechanically Induced Overstrain," Experimental Mechanics, Vol. 3, 1963, pp. 253-262.

[6]Milligan, R. V., Koo, W. H., and Davidson, T. E., "The Bauschinger Effect in a High-Strength Steel," Journal of Basic Engineering, Transactions ASME, Vol. 88, 1966, pp. 480-488.

stress relative to yield strength is reduced from the ideal value of 0.85 to 0.53. Such effects of compressive strength reduction on residual stress and thus indirectly on fatigue crack growth rate and fatigue life, are described further in an upcoming section.

The effect of residual stress, including the appropriate compressive strength reduction, on brittle failure of the redesigned cannon can be determined as follows. From Figure 4, for 50% overstrain which was used in redesign and for the relatively shallow crack depth of the prior failure, $r/r_1 = 1.10$, the residual stress is 0.38 times the yield strength, $\sigma_{\theta-R} = -390$ MPa. This value* can be used in a modification of Equation (1) to obtain an approximate K expression which includes the effect of residual stress,

$$K = f_p f_s\, p(\pi a)^{1/2} + 1.12\, f_s\, \sigma_{\theta-R}(\pi a)^{1/2} \qquad (4)$$

Using $\sigma_{\theta-R} = -390$ MPa and with all other values as before, the applied K with residual stress present is significantly reduced, see Figure 2. This, combined with an increased K_{Ic}, makes failure at such small crack depth ($a = 0.1W$) quite unlikely. Failure at a deep crack is still possible, but for a deep crack for which the benefits of residual stress diminish, the loss of plane-strain constraint as the crack approaches the outer radius causes an increase in effective fracture toughness. This will tend to compensate for the loss of benefit from residual stress. Of course, the proof of the redesign is in the experience. Since the redesign of the 175 mm cannon to the material property and residual stress conditions indicated in Figure 2, there

*This value is correct for a cylinder with $r_2/r_1 = 2.00$, whereas the cannon being considered has $r_2/r_1 = 2.09$. The difference between the two results will have no effect on conclusions drawn from the analysis.

have been no further brittle failures, even after many times the number of firing cycles of the early failure.

TEST METHOD DEVELOPMENT

The importance of fracture toughness testing to the structural integrity of high strength pressure vessels is apparent from the preceding discussion. When brittle fracture is possible, fracture toughness testing is essential. In reaction to this, a new fracture specimen has been developed which is uniquely suited to cylindrical pressure vessels.[7] First called the C-shaped specimen, more recently the arc specimen, it is now used worldwide and is part of ASTM Method E-399 for Plane-Strain Fracture Toughness of Metallic Materials.[8]

The arc specimen is shown in Figure 5 along with the dashed outline of the rectangularly shaped compact specimen. By using the full wall thickness of a cylinder, the arc specimen both saves fabrication time and yields a larger effective specimen depth, W, than does a rectangular specimen taken from the same cylinder.

The development of the arc specimen included boundary value collocation and experimental compliance stress intensity factor, K, analyses of prospective geometries by three different laboratories.[9] A sample of results

---

[7] Kendall, D. P. and Hussain, M. A., "A New Fracture Toughness Test Method for Thick-Walled Cylinder Material," Experimental Mechanics, Vol. 12, 1972, pp. 184-189.

[8] "Standard Test Method For Plane-Strain Fracture Toughness of Metallic Materials," E-399, Annual Book of ASTM Standards, Part 10, American Society for Testing and Materials, 1981, pp. 588-618.

[9] Underwood, J. H. and Kendall, D. P., "Fracture Toughness Testing Using the C-Shaped Specimen," Developments in Fracture Mechanics Test Methods Standardization, ASTM STP 632, W. F. Brown, Jr. and J. G. Kaufman, Eds., American Society for Testing and Materials, 1977, pp. 25-38.

from these analyses is shown in Figure 6. In general, and as shown in Figure 6, the agreement between the collocation results from two different laboratories and methods was excellent, within a few tenths of a percent. The good agreement, within a few percent, between the experimental compliance K values and those from collocation is a further independent check on the stress and K analyses of the arc specimen.

Polynomial expressions have been developed to represent the collocation results while still converging to the exact limit solution for shallow and deep cracks. A recent extension of an earlier expression is accurate within ± three percent over a wide range of geometry* for arc specimens and is part of ASTM Method E399. It is[10]

$$\frac{KBW^{1/2}}{P} = \left[\frac{3X}{W} + 1.9 + 1.1\,\frac{a}{W}\right]\left[1 + 0.25\left(1 - \frac{a}{W}\right)^2\left(1 - \frac{r_1}{r_2}\right)\right]\left[\frac{\left(\frac{a}{W}\right)^{1/2}}{\left(1 - \frac{a}{W}\right)^{3/2}}\right] \cdot \left[3.74 - 6.30\,\frac{a}{W} + 6.32\left(\frac{a}{W}\right)^2 - 2.43\left(\frac{a}{W}\right)^3\right] \qquad (5)$$

for $0.2 \leq \frac{a}{W} \leq 1$, $0 \leq \frac{r_1}{r_2} \leq 1.0$, $0 \leq \frac{X}{W} \leq 1.0$.

The key to a wide range K expression, as discussed by Srawley,[11] is attention to deep crack limit solutions. For the arc specimen the important solution is bending of the uncracked ligament ahead of a deep crack approach-

---

[10] Kapp, J. A., Newman, J. C., Jr., and Underwood, J. H., "A Wide Range Stress Intensity Factor Expression For the C-Shaped Specimen," Journal of Testing and Evaluation, Vol. 8, 1980, pp. 314-317.

[11] Srawley, J. E., "Wide Range Stress Intensity Factor Expressions for ASTM E-399 Standard Fracture Toughness Specimens," International Journal of Fracture Mechanics, Vol. 12, 1976, pp. 475-476.

*For the specific geometries of K_{Ic} testing, the expression is accurate within ± one percent.

ing a free surface, in this case the outer radius. In the terminology here, the deep crack limit K is:

$$\frac{KBW^{1/2}}{P} = \frac{3.975\left[\frac{X}{W} + \frac{1}{2} + \frac{a}{2W}\right]}{\left(1 - \frac{a}{W}\right)^{3/2}} \qquad (6)$$

where the bracketed term is the bending moment arm for the arc specimen.

The form and constants of Equation (6) and a similar tension limit solution were used in developing the wide range K expression for the arc specimen. Because K converges to the proper deep crack limit, the specimen can be used for fatigue crack growth tests and other fracture mechanics tests which involve deep cracks. The arc specimen can also be used for J-integral tests to measure J_{Ic} and for tests involving bending loads, although specific procedures for these tests have not been well documented yet.

EXAMPLES OF FRACTURE ANALYSIS

Fracture of pressure vessels can be categorized using three basic types of crack growth: fast crack growth, environmentally assisted crack growth, and fatigue crack growth. A recent example of each type of crack growth in cannons is given here to illustrate current applications of fracture mechanics to cylindrical pressure vessels.

Fast Fracture

The beneficial effect of lowering the yield strength in preventing fast, brittle fracture was included in the discussion of the early failure. The strength level effect is so basic to fracture concerns with pressure vessels

that it should be considered further. Figure 7 shows test results from eight different types of forged cylindrical pressure vessels,[12] some for prototype cannons, some for research purposes. The material is the ASTM A723 steel discussed earlier, with vacuum processing used in all cases. The vacuum processing and the prototype nature of the forgings combine to give fracture toughness values which are near the upper limit for this class of material. Nevertheless, the results show clearly the typical decrease in toughness which is obtained with an increase in yield strength. This is a consistent trend for the ASTM K_{Ic} measurements, for K_{Ic} measurements with a smaller than required specimen size, and for K_{Ic} calculated from the result of J-integral, J_{Ic} tests. The linear regression line and ± 10 percent limits show that, only for the material and strength range here, there is an inverse linear relation between toughness and strength with relatively little scatter. The variation of -40°C notched impact charpy energy with room temperature yield strength is also shown in Figure 7 for six of the eight types of forgings. Again, an inverse relation exists between charpy energy as a measure of toughness and yield strength. Note that it is not a linear inverse relation, so linear correlations between charpy energy and K_{Ic} should not be attempted.

The likelihood of fast cracking is certainly affected by factors other than the material fracture toughness. A recent experience with a pressure vessel demonstrates the effects of crack shape and tensile residual stress on

---

[12]Underwood, J. H., "The Equivalence of K_{Ic} and J_{Ic} Fracture Toughness Measurements in Ni-Cr-Mo Steels," Experimental Mechanics, Vol. 18, 1978, pp. 350-355.

fast cracking. A 1.5 m long, overstrained cylinder with r_1 = 79 mm and r_2 = 142 mm was cyclically pressurized with oil from 0 to 386 MPa. A fatigue crack initiated at a 10 mm deep, 25 mm wide, 550 mm long longitudinal notch on the outer diameter. The fatigue crack grew to the critical size at which K_{Ic} controlled fast cracking occurred. The resulting failure did not involve fragmentation, so it was not a brittle failure in that sense, but neither was it a leak-before-break failure. Figure 8 shows a portion of the fracture surface, as well as the distribution of overstrain residual stress present in the cylinder before fracture. The maximum depth of the notch plus the critical fatigue crack was 16 mm, only about one quarter of the cylinder wall thickness when fast fracture of the remaining wall thickness and the entire cylinder length occurred.

Fast fracture from such a shallow crack was affected by (1) the tensile residual stress in the outer portion of the cylinder due to the 100% overstrain, and (2) the long, straight-fronted crack shape due to the notch. A measure of the effect on the applied K of these two factors can be obtained from an expression for K for an OD crack in the cylinder. The expression is obtained using an approach similar to that for Equation (4):

$$K = 1.12\ f_s\ (\sigma_{\theta-R} + \sigma_{0-p})(\pi a)^{1/2} \qquad (7)$$

The shape factor, f_s, has a value very near 1.0, because the crack is essentially straight-fronted. So the reduction in K associated with the more usual semielliptical shaped crack is not present in this case due to the longitudinal notch. The tensile residual stress at the location of the critical crack, $\sigma_{\theta-R}$, can be estimated from Figure 4 as about 0.22 times the yield strength, 1230 MPa. This estimate, 270 MPa, takes into account the

reduced compressive yield strength discussed earlier and the fact that r_2/r_1 = 1.8 for this cylinder. The tensile applied stress in the cylinder can be calculated from the well known relation for a cylinder:[13]

$$\sigma_{\theta-p} = \frac{p[1 + (r_2/r)^2]}{(r_2/r_1)^2 - 1} \qquad (8)$$

In the above r_2/r = 1.13 for a crack one quarter through the wall, and $\sigma_{\theta-p}$ = 391 MPa.

Applying the above values of f_s, $\sigma_{\theta-R}$ and $\sigma_{\theta-p}$ to Equation (7), along with a = 16 mm = 0.016 m, gives an applied K = 166 MPa$\cdot m^{1/2}$. This is somewhat above the K_{Ic} value from the cylinder material, 162 MPa$\cdot m^{1/2}$, so the fast failure would not be unexpected. The important point is that both the crack shape and residual stresses had significant contributions to the fast fracture. These factors must be reckoned with in the fracture analysis of pressure vessels.

Environmental Fracture

Environmentally assisted fracture is an important consideration in pressure vessels because three basic requirements for this type of fracture are often present, susceptible material, sustained tensile loading, and aggressive environment. Pressure vessels are often made of high strength materials, many of which are susceptible to environmentally assisted fracture. Long time applied or residual stresses are common in pressure vessels. Fluids which may be aggressive are contained.

---

[13]Timoshenko, S. and MacCullough, G. H., Elements of Strength of Materials, D. Van Nostrand Co., Princeton, NJ, 1949, p. 26.

The above three requirements were present and led to a recent example of stress corrosion cracking in a cannon tube. The high strength steel alloy is susceptible to stress corrosion cracking in certain environments. The sustained tensile loading present in this case is believed to be tensile residual stress which was caused by compressive yielding resulting from the combination of thermal and overstrain stresses at the inner radius of the tube. The environment was the firing products which include hydrogen sulfide, a highly aggressive environment for stress corrosion cracking in many steels.

The stress corrosion cracking of the cannon tube is described by two photomicrographs. Figure 9a is a cross-section of a piece of a tube in which cracking has occurred. The section is lightly shaded due to the metallographic polish. It contains two rifling lands at the inner radius. The primary crack started at the corner of a rifling land, grew by mixed stress corrosion and fatigue cracking (location 1), and then grew in the radial direction by mixed fatigue and fast cracking (location 2) out toward the outer radius and a leak-before-break failure. A smaller crack at a rifling land (location 3) is shown at higher magnification in Figure 9b. The classic, multiply-branched cracking is a clear indication of stress corrosion cracking. Figure 10 shows scanning electron microscope fractographs which compare the stress corrosion, fatigue, and fast fracture regions and further confirm that the initiation and primary cause of the failure was environmentally assisted fracture.

This environmentally controlled failure in a gun tube occurred after several years of service, and the final failure was safe and contained. The delay in environmentally assisted failure nearly always occurs; the safe final condition does not. Whenever the combination of sustained loading and an

unsuitable material/environment couple is present in a pressure vessel, environmentally assisted failure must be considered.

Fatigue Fracture

Repeated application of pressure to vessels provides the means whereby cracks, which initiate due to stress concentrations or service environments, can grow to the critical size required for fast fracture. This is a common sequence of events for cannon pressure vessels. Often the fatigue crack growth process is most of the life of a cannon, so considerable fatigue life testing and associated analysis of cannons has been performed. References 14, 15, and 16 are examples. Much of the life testing and analysis has centered on the two factors already discussed here, crack shape and residual stress. With the recent comprehensive work of Newman and Raju,[3] the effects of crack shape on K and thus on cracking and fatigue life can be well characterized. Also, many investigators are now addressing the second factor, the effects of residual stress on life. In demonstration of this, a new ASTM subcommittee has recently been formed, E9.02, Residual Stress Effects in Fatigue.

---

[3]Newman, J. C., Jr., and Raju, I. S., "An Empirical Stress-Intensity Factor Equation for the Surface Crack," Engineering Fracture Mechanics, Vol. 15, 1981, pp. 185-192.

[14]Davidson, T. E., Brown, B. B., and Kendall, D. P., "Materials and Processes Considerations in the Design of Pressure Vessels," High Pressure Engineering, H.L.I.D. Pugh, Ed., The Institution of Mechanical Engineers, 1977, pp. 63-71.

[15]Davidson, T. E. and Throop, J. F., "Practical Fracture Mechanics Applications to Design of High Pressure Vessels," Application of Fracture Mechanics to Design, J. J. Burke and V. Weiss, Eds., Plenum Publishing Corp., New York, 197^, pp. 111-138.

[16]Parker, A. P., Underwood, J. H., Throop, J. F., and Andrasic, C. P., "Stress Intensity and Fatigue Crack Growth in a Pressurized Autofrettaged Thick Cylinder," submitted to Proceedings of 14th National Symposium on Fracture Mechanics, Los Angeles, June 1981.

The work of Parker et al[16] specifically addresses the effects of residual stress on the life of cannon pressure vessels. They developed K expressions for pressurized cylinders with overstrain residual stress, and they numerically integrated da/dN versus ΔK expressions to calculate life as affected by residual stress. Comparison of calculated with actual lives led them to conclude that accurate determination of the residual stress actually present in a cylinder is required for reliable life calculations. A reexamination of Figure 4 will support this conclusion. In all the plots shown, the compressive stress is significant relative to yield strength near the inner radius, where much of the fatigue life is expended. Thus, the correctness of this residual stress will have a large effect on the calculated life, and a small change in this stress can have a much magnified effect on the actual life, because there is a near balance between applied tension and residual compression stress. In the following last example of fracture mechanics analysis of cylindrical pressure vessels, an estimate of the actual residual stress distribution in an overstrained cylinder and its effect on fatigue life will be described. Comparison will be made between calculated fatigue life and laboratory measurements[16] from full size cylinders.

First, an estimate of the actual residual stress distribution in an overstrained cylinder is made, as opposed to an analysis which assumes ideal elastic unloading of a cylinder during overstrain. Milligan[6] showed that A723

---

[6]Milligan, R. V., Koo, W. H., and Davidson, T. E., "The Bauschinger Effect in a High-Strength Steel," Journal of Basic Engineering, Transactions ASME, Vol. 88, 1966, pp. 480-488.

[16]Parker, A. P., Underwood, J. H., Throop, J. F., and Andrasic, C. P., "Stress Intensity and Fatigue Crack Growth in a Pressurized Autofrettaged Thick Cylinder," submitted to Proceedings of 14th National Symposium on Fracture Mechanics, Los Angeles, June 1981.

type steels, following tensile plastic deformation, exhibit a reduction in compressive strength properties, called the Bauschinger effect. For the situation here, the overstrain of a cylinder, Figure 11 summarizes this effect. The plot is an estimate of the effective stress versus strain history at the inner radius of an $r_2/r_1 = 2.0$ cylinder as it undergoes a 100% overstrain procedure. Davidson et al[17] calculated the tensile plastic deformation for these conditions to be 1.01%. For this amount of tensile plastic deformation, the reduced compressive yield properties[6] are compared with linear unloading in Figure 11. Using the reduced properties, corrected values of overstrain residual stress in a cylinder can be obtained. For example, from Figure 11 the value of circumferential residual stress at the inner radius, $\sigma_{\theta-R}$, for ideal linear unloading is 0.85 times the unaffected yield strength, or 1000 MPa in this case. When the reduced compressive yield properties are used, the corrected value is 620 MPa. Applying such corrected values of compressive yield strength to several points in the compressive residual stress region of the overstrained cylinder gives the corrected residual stress distribution plots shown in Figure 4. The tensile portion of the corrected plots in Figure 4 was obtained by reducing the total area above zero stress in the tension portion by the same ratio as that obtained in the compression portion.

A proof of a corrected residual stress distribution is to use it to calculate fatigue life for comparison with experiment. This was done and is

---

[6]Milligan, R. V., Koo, W. H., and Davidson, T. E., "The Bauschinger Effect in a High-Strength Steel," Journal of Basic Engineering, Transactions ASME, Vol. 88, 1966, pp. 480-488.

[17]Davidson, T. E., Barton, C. S., Reiner, A. N., and Kendall, D. P., "Overstrain of High-Strength Open-End Cylinders of Intermediate Diameter Ratio," Proceedings of the First International Congress on Experimental Mechanics, Pergamon Press, Oxford, 1963, pp. 335-352.

summarized in Figures 12 and 13. Fatigue life calculations were made for the conditions of recent fatigue life experiments,[16] 0% and 60% overstrained cylinders with $r_2/r_1 = 2.0$, $r_1 = 90$ mm, yield strength = 1175 MPa, internal pressure $p = 331$ MPa, and a semicircular starter notch with initial depth $a_i =$ 6.4 mm. Figure 12 shows the residual stress distribution calculated from Equations (2) and (3) which assume ideal elastic unloading. Also shown is the distribution corrected for reduced compressive strength, using the method described in relation to Figures 4 and 11. The compressive residual stress at the inner radius, $\sigma_{\theta-R}$ for $r = r_1$, is decreased from -860 MPa to -600 MPa by the correction.

The ideal and corrected stress distributions shown in the lower plot of Figure 12 are used to obtain K distributions for a pressurized, overstrained tube using the following general expression[4]

$$K/\sigma_o(\pi a)^{1/2} = 1.12 - 0.68(a/a_o) \qquad (9)$$

Equation (9) is a short crack K expression for a linear varying stress distribution in which σ_o is the stress for $a = 0$, that is, at the edge of the specimen, and a_o is the crack length for $\sigma = 0$, that is, for the point where the stress distribution crosses the zero stress line. Equation (9) can be applied to the nearly linear stress distributions in Figure 12 by letting $\sigma_o = \sigma_{\theta-R}$ (for $r = r_1$) and $a_o = 0.38$ W, that is, $r/r_1 = 1.38$. Doing so and

---

[4]Underwood, J. H. and Throop, J. F., "Surface Crack K-Estimates and Fatigue Life Calculations in Cannon Tubes," Part-Through Crack Fatigue Life Prediction, ASTM STP 587, J. B. Chang, Ed., American Society for Testing and Materials, 1979, pp. 195-210.

[16]Parker, A. P., Underwood, J. H., Throop, J. F., and Andrasic, C. P., "Stress Intensity and Fatigue Crack Growth in a Pressurized Autofrettaged Thick Cylinder," submitted to Proceedings of 14th National Symposium on Fracture Mechanics, Los Angeles, June 1981.

combining the resulting K distribution for compressive stress with that from the applied tensile loading due to pressure[2] gives the total K distributions shown in the upper plot of Figure 12. Note that the total K, based on ideal elastic unloading, nearly vanishes for $r = r_1$, whereas the total K corrected for reduced compressive stress is significantly higher. This has a significant effect on fatigue life.

Fatigue life can be calculated from a known K distribution by integration of a Paris-Erdogan[18] type equation:

$$da/dN = C\,\Delta K^3 \qquad (10)$$

where C is a material constant from fatigue growth rate tests, and the power 3 is often a good representation for steels. For applications in which the minimum load is either compression or zero, as is the case here, ΔK is equivalent to the maximum K. If it can be assumed that the simple K parameter, $f_k = K/p(\pi a)^{1/2}$, remains constant, the integration of Equation (10) is simple. Referring again to Figure 12, f_k is nearly constant for K due to pressure only, but is less so for total K. Nevertheless, a constant value of f_k will be used here with the rationale that the selection of a representative, average f_k will provide a consistent, readily understandable method for calculating fatigue life. Taking this approach, the integration of Equation (10) gives

$$N = \frac{2(a_i^{-1/2} - a_f^{-1/2})}{C(f_k f_s\, p\pi^{1/2})^3} \qquad (11)$$

---

[2]Bowie, O. L. and Freese, C. E., "Elastic Analysis For a Radial Crack in a Circular Ring," Engineering Fracture Mechanics, Vol. 4, 1972, pp. 315-321.

18Paris, P. C. and Erdogan, F., "A Critical Analysis of Crack Propagation Laws," Journal of Basic Engineering, Transactions ASME, Vol. 85, 1963, pp. 528-534.

where N is the number of pressure cycles required to grow a crack from an initial to a final crack depth, a_i to a_f. Calculations of N were made using the following values in Equation (11): a_i = 0.0064 m; a_f = 0.090 m, the full wall thickness; C = 6.52 x 10^{-12} $cycle^{-1}$ MPa^{-3} $m^{-1/2}$, the value from growth rate tests; p = 331 MPa; f_k = 2.76 for 0% overstrain, 1.37 for 60% corrected, 1.00 for 60% ideal; f_s = 0.53. The values of f_k were taken from Figure 12 for r/r_1 = 1.2, which was selected by engineering judgment as the crack depth, a/W = 0.2, which gives a representative value of K for describing fatigue life. The value of f_s was taken from Reference 3 for this crack depth, a/W = 0.2, and the semicircular shape, a/2c = 0.5.

The comparison of calculated with experimental a versus N curves is shown in Figure 13. The experimental curves are based on crack depth measurements using an ultrasonic method and on markings observed on the fracture surface after the tests. The crack shape remained nearly semicircular throughout both tests. The calculated curves for 0% overstrain and 60% overstrain with ideal elastic unloading result in about the same comparison with experiment as observed in the numerical calculations of Parker et al,[16] that is, the 0% calculation is less than half of the experimental life and the 60% ideal calculation is more than twice the experimental life. The calculated curve for 60% overstrain with correction for reduced compressive strength agrees

---

[3]Newman, J. C., Jr., and Raju, I. S., "An Empirical Stress-Intensity Factor Equation for the Surface Crack," Engineering Fracture Mechanics, Vol. 15, 1981, pp. 185-192.

[16]Parker, A. P., Underwood, J. H., Throop, J. F., and Andrasic, C. P., "Stress Intensity and Fatigue Crack Growth in a Pressurized Autofrettaged Thick Cylinder," submitted to Proceedings of 14th National Symposium on Fracture Mechanics, Los Angeles, June 1981.

much better with experiment and, in addition, is more consistent because it underpredicts the experimental life as does the 0% calculation. In summary, the proposed correction accounts for the known reduction in compressive strength of the material, and it also gives better and more consistent agreement between calculated and experimental fatigue life.

REFERENCES

1. Davidson, T. E., Throop, J. F. and Underwood, J. H. "Failure of a 175 MM Cannon Tube and the Resolution of the Problem Using an Autofrettage Design," Case Studies in Fracture Mechanics, T. P. Rich and D. J. Cartwright, Eds., AMMRC MS 77-5, Army Materials and Mechanics Research Center, 1977.

2. Bowie, O. L., and Freese, C. E., "Elastic Analysis For a Radial Crack In Circular Ring," Engineering Fracture Mechanics, Vol. 4, 1972, pp. 315-321.

3. Newman, J. C. Jr., and Raju, I. S., "An Empirical Stress-Intensity Factor Equation for the Surface Crack," Engineering Fracture Mechanics, Vol. 15, 1981, pp. 185-192.

4. Underwood, J. H. and Throop, J. F., "Surface Crack K-Estimates and Fatigue Life Calculations in Cannon Tubes," Part-Through Crack Fatigue Life Prediction, ASTM STP 587, J. B. Chang, Ed., American Society for Testing and Materials, 1979, pp. 195-210.

5. Davidson, T. E., Kendall, D. P., and Reiner, A. N., "Residual Stresses in Thick-Walled Cylinders Resulting From Mechanically Induced Overstrain," Experimental Mechanics, Vol. 3, 1963, pp. 253-262.

6. Milligan, R. V., Koo, W. H., and Davidson, T. E., "The Bauschinger Effect in a High-Strength Steel," Journal of Basic Engineering, Transactions ASME, Vol. 88, 1966, pp. 480-488.

7. Kendall, D. P. and Hussain, M. A., "A New Fracture Toughness Test Method for Thick-Walled Cylinder Material," Experimental Mechanics, Vol. 12, 1972, pp. 184-189.

8. "Standard Test Method For Plane-Strain Fracture Toughness of Metallic Materials," E-399, Annual Book of ASTM Standards, Part 10, American Society For Testing and Materials, 1981, pp. 588-618.

9. Underwood, J. H. and Kendall, D. P., "Fracture Toughness Testing Using the C-Shaped Specimen," Developments in Fracture Mechanics Test Methods Standardization, ASTM STP 632, W. F. Brown, Jr. and J. G, Kaufman, Eds., American Society for Testing and Materials, 1977, pp. 25-38.

10. Kapp, J. A., Newman, J. C. Jr., and Underwood, J. H., "A Wide Range Stress Intensity Factor Expression For the C-Shaped Specimen," Journal of Testing and Evaluation, Vol. 8, 1980, pp. 314-317.

11. Srawley, J. E., "Wide Range Stress Intensity Factor Expressions for ASTM E-399 Standard Fracture Toughness Specimens," International Journal of Fracture Mechanics, Vol. 12, 1976, pp. 475-476.

12. Underwood, J. H., "The Equivalence of K_{Ic} and J_{Ic} Fracture Toughness Measurements in Ni-Cr-Mo Steels," Experimental Mechanics, Vol. 18, 1978, pp. 350-355.

13. Timoshenko, S., and MacCullough, G. H., Elements of Strength of Materials, D. Van Nostrand Co., Princeton, NJ, 1949, p. 26.

14. Davidson, T. E., Brown, B. B., and Kendall, D. P., "Materials and Processes Considerations in the Design of Pressure Vessels," High Pressure Engineering, H.L.I.D. Pugh, Ed., The Institution of Mechanical Engineers, 1977, pp. 63-71.

15. Davidson, T. E. and Throop, J. F., "Practical Fracture Mechanics Applications to Design of High Pressure Vessels," Application of Fracture Mechanics to Design, J. J. Burke and V. Weiss, Eds., Plenum Publishing Corp., New York, 1979, pp. 111-138.

16. Parker, A. P., Underwood, J. H., Throop, J. F., and Andrasic, C. P., "Stress Intensity and Fatigue Crack Growth in a Pressurized Autofrettaged Thick Cylinder," submitted to proceedings of 14th National Symposium on Fracture Mechanics, Los Angeles, June 1981.

17. Davidson, T. E., Barton, C. S., Reiner, A. N., and Kendall, D. P., "Overstrain of High-Strength Open-End Cylinders of Intermediate Diameter Ratio," Proceedings of the First International Congress on Experimental Mechanics, Pergamon Press, Oxford, 1963, pp. 335-352.

18. Paris, P. C., and Erdogan, F., "A Critical Analysis of Crack Propagation Laws," Journal of Basic Engineering, Transactions ASME, Vol. 85, 1963, pp. 528-534.

Figure 1. Brittle Failure of 175 mm Cannon Tube.

FIGURE 2

FAILURE AND REDESIGN OF 175 MM CANNON TUBE

GEOMETRY; LOADING

R_1 = 89 MM, R_2 = 186 MM; R_2/R_1 = 2.09

P = 345 MPA, CYCLIC LOADING

FAILURE CONDITIONS

MATERIAL: σ_{YS} = 1180 MPA; IMPACT ENERGY = 7J;

K_{IC} = 90 MPA·M$^{1/2}$

CRITICAL CRACK SIZE: A_C = 9.4 MM; $A_C/2C$ = 0.33; A_C/W = 0.10

RESIDUAL STRESS: $\sigma_{\theta-R}$ = 0

APPLIED K: $K = F_{P(R_2/R_1, A/W)}\ F_{S(A/2C, A/W)}\ P\sqrt{\pi A}$

K = 112 MPA·M$^{1/2}$

$K_{APPLIED} > K_{IC}$; FAILURE EXPECTED

REDESIGN CONDITIONS

MATERIAL: σ_{YS} = 1030 MPA; IMPACT ENERGY = 34J;

K_{IC} = 137 MPA·M$^{1/2}$

RESIDUAL STRESS: $\sigma_{\theta-R}$ = -520 MPA AT R = R_1

= -390 MPA AT R = R_1 + 0.1W

APPLIED K:

FOR SHALLOW CRACKS:

$$K = F_{P(R_2/R_1, A/W)}\ F_{S(A/2C, A/W)}\ P\sqrt{\pi A} + 1.12\ F_{S(A/2C, A/W)}\ \sigma_{\theta-R}\sqrt{\pi A}$$

FOR A = 0.10W:

K = 112 - 52 = 60 MPA·M$^{1/2}$

$K_{APPLIED} < K_{IC}$; FAILURE NOT EXPECTED

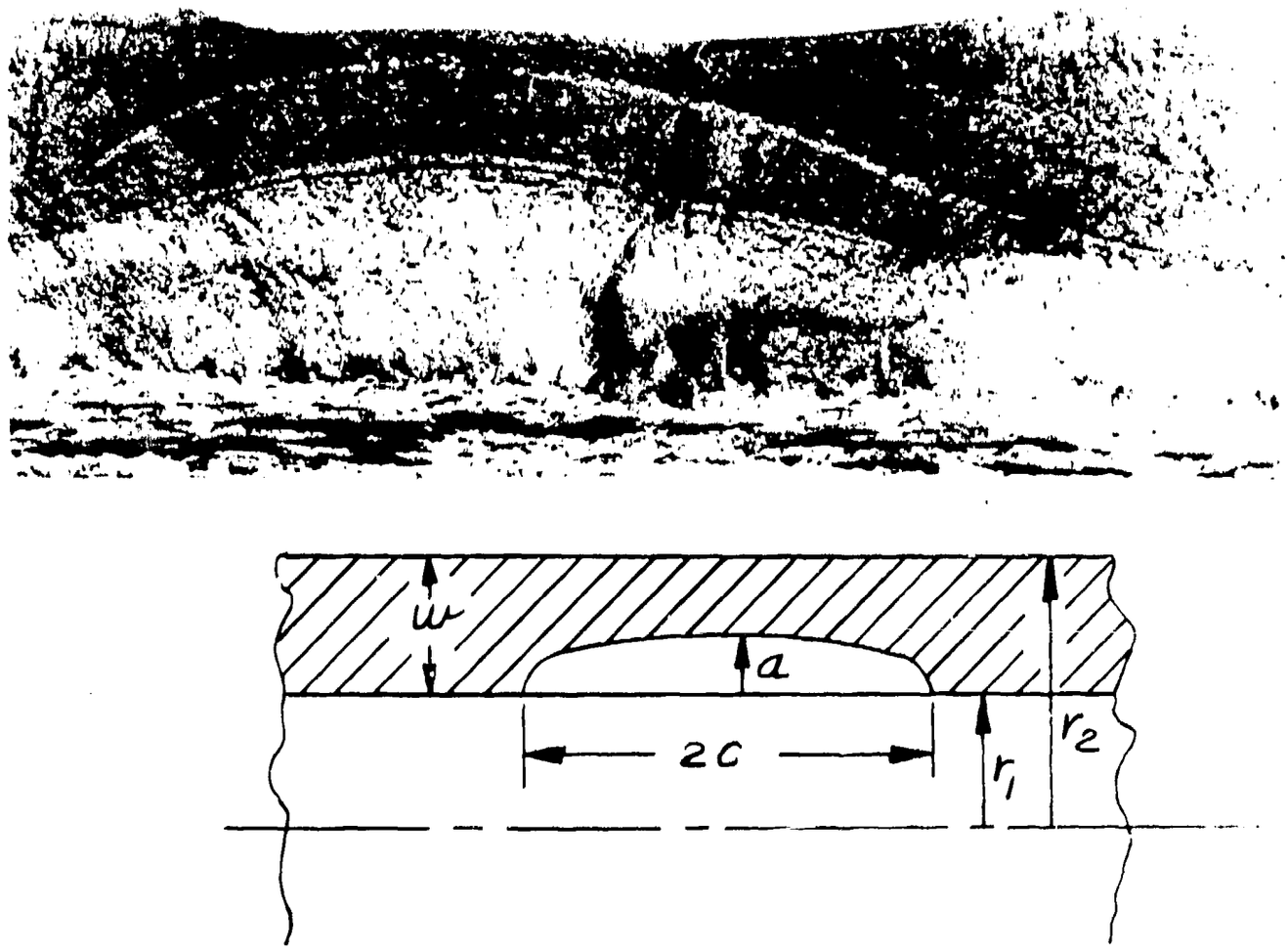

Figure 3. Contained Leak-Before-Break Cracking in a Cannon.

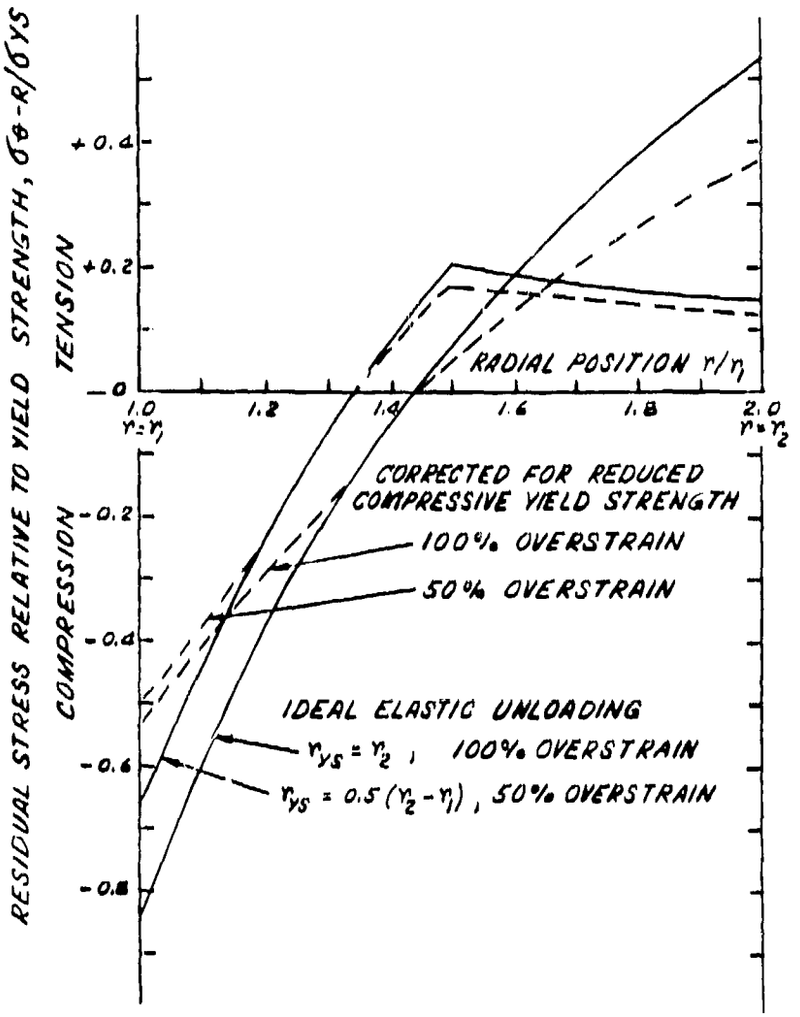

Figure 4. Circumferential Residual Stress Distributions for Overstrained Cylinders with $r_2/r_1 = 2.0$.

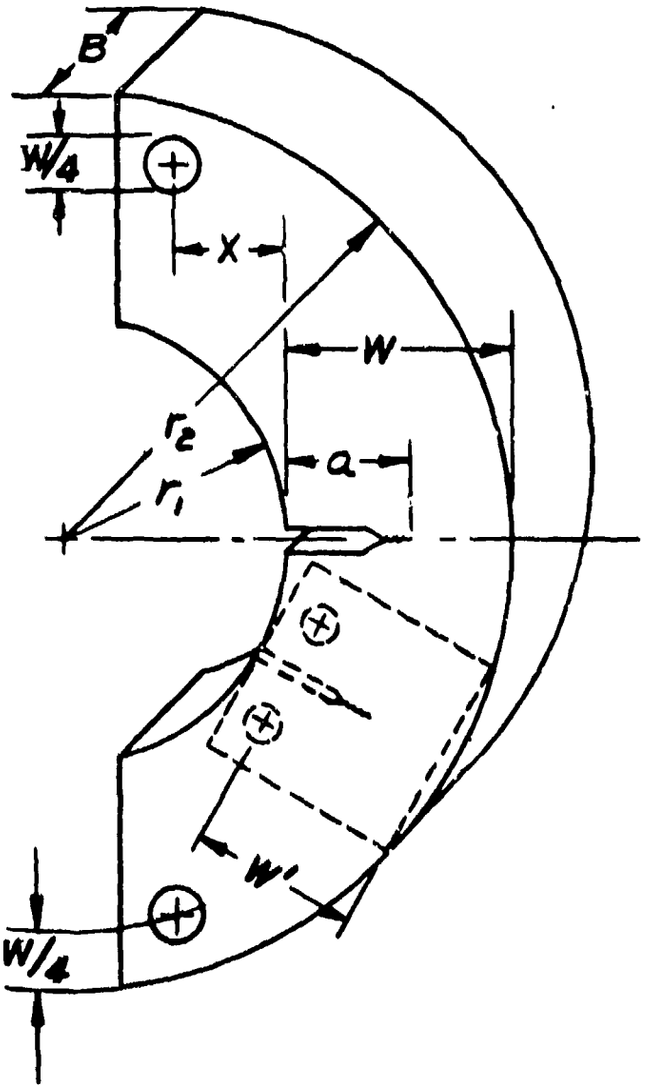

Figure 5. Arc Specimens for Fracture Mechanics Tests of Material in Hollow Cylinder Geometries.

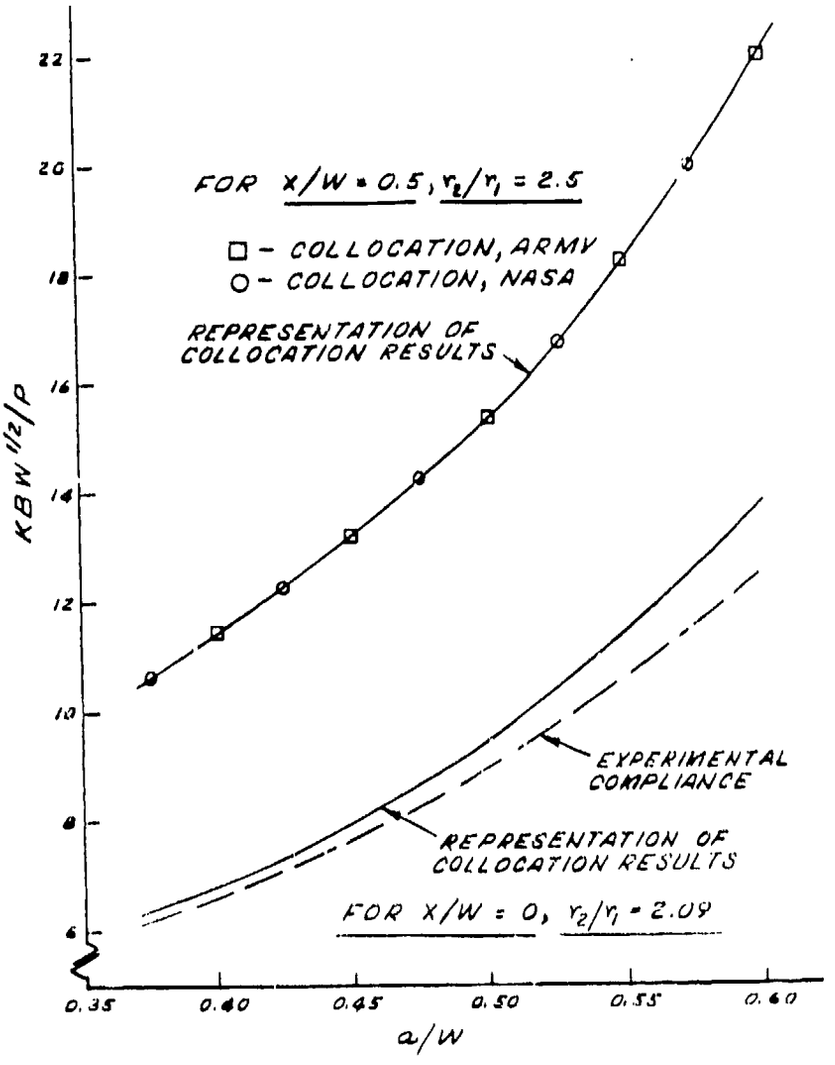

Figure 6. Stress Intensity Factor, K, Results for Arc Specimen from Experiment and Analysis.

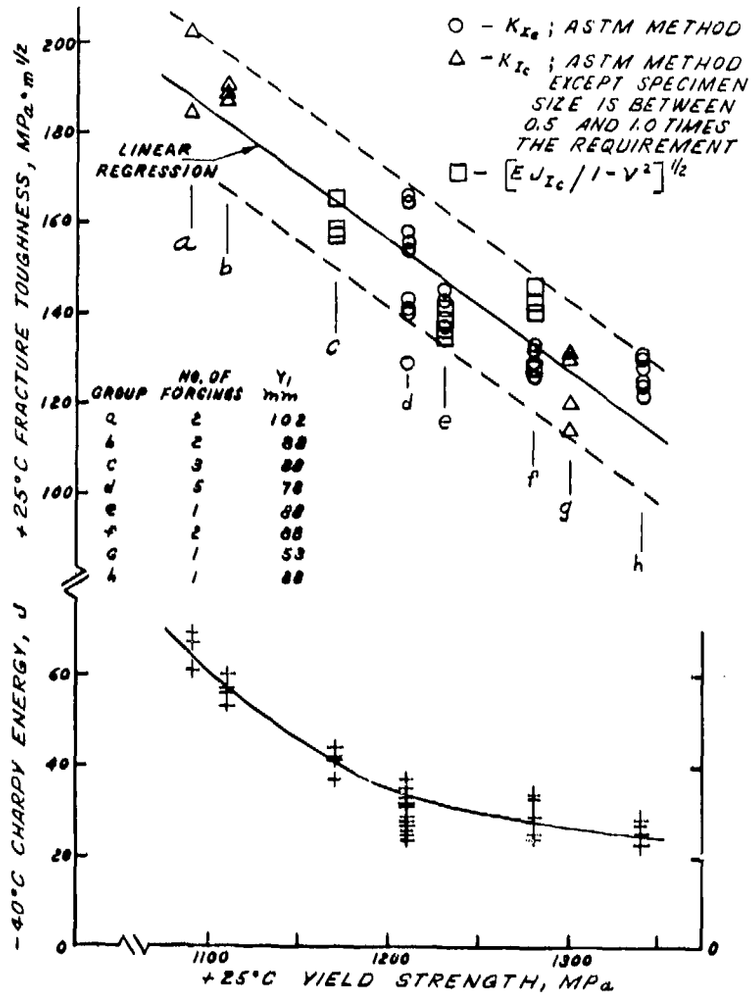

Figure 7. Variation of Fracture Toughness with Yield Strength for Ni-Cr-Mo-V Steel Forgings.

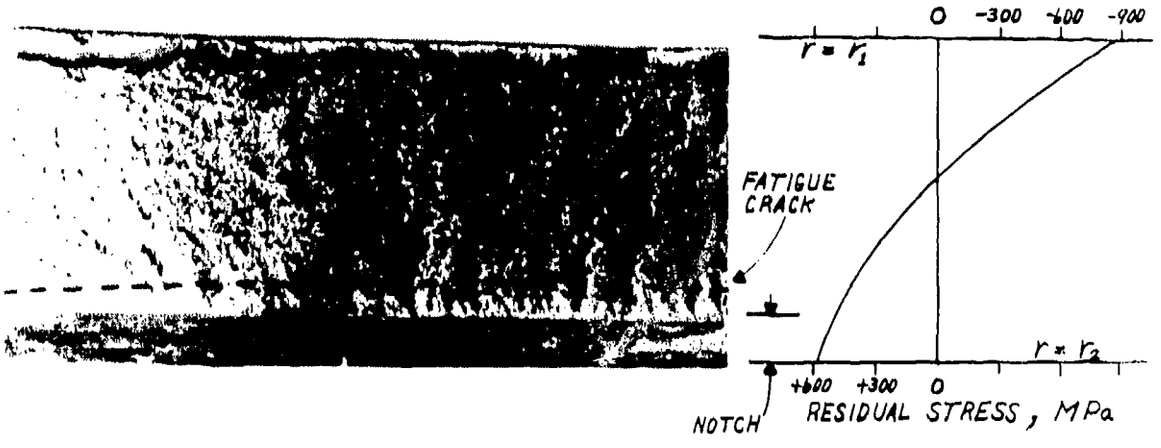

Figure 8. Fast Fracture Affected by Crack Shape and Tensile Residual Stress.

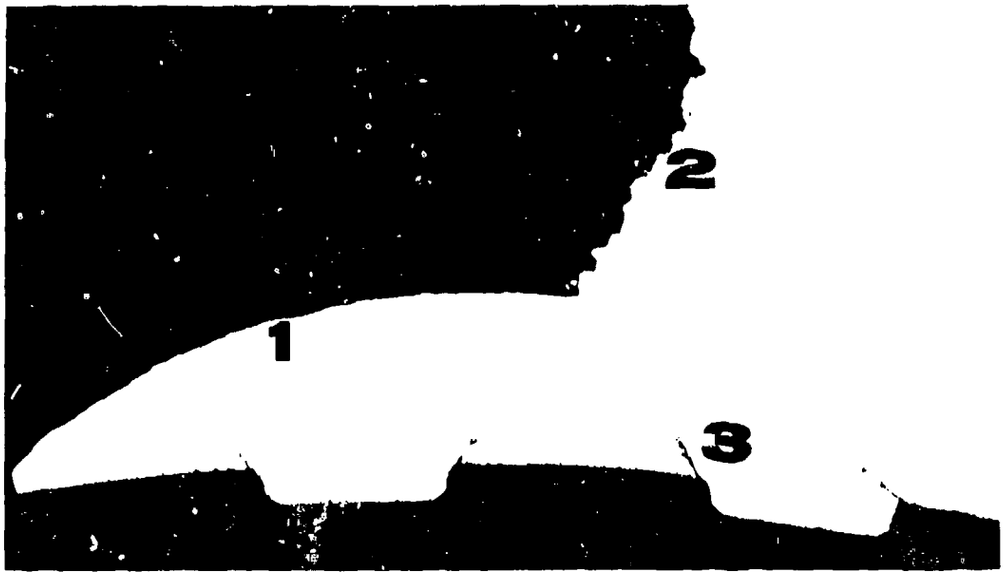

(a) Location 1 - Mixed Stress Corrosion and Fatigue Cracking;
Location 2 - Fast Fracture;
Location 3 - Initiation of Stress Corrosion Cracking at Rifling Land; 15X

(b) Micrograph of Location 3, 100X.

Figure 9. Stress Corrosion Cracking in a Cannon Tube.

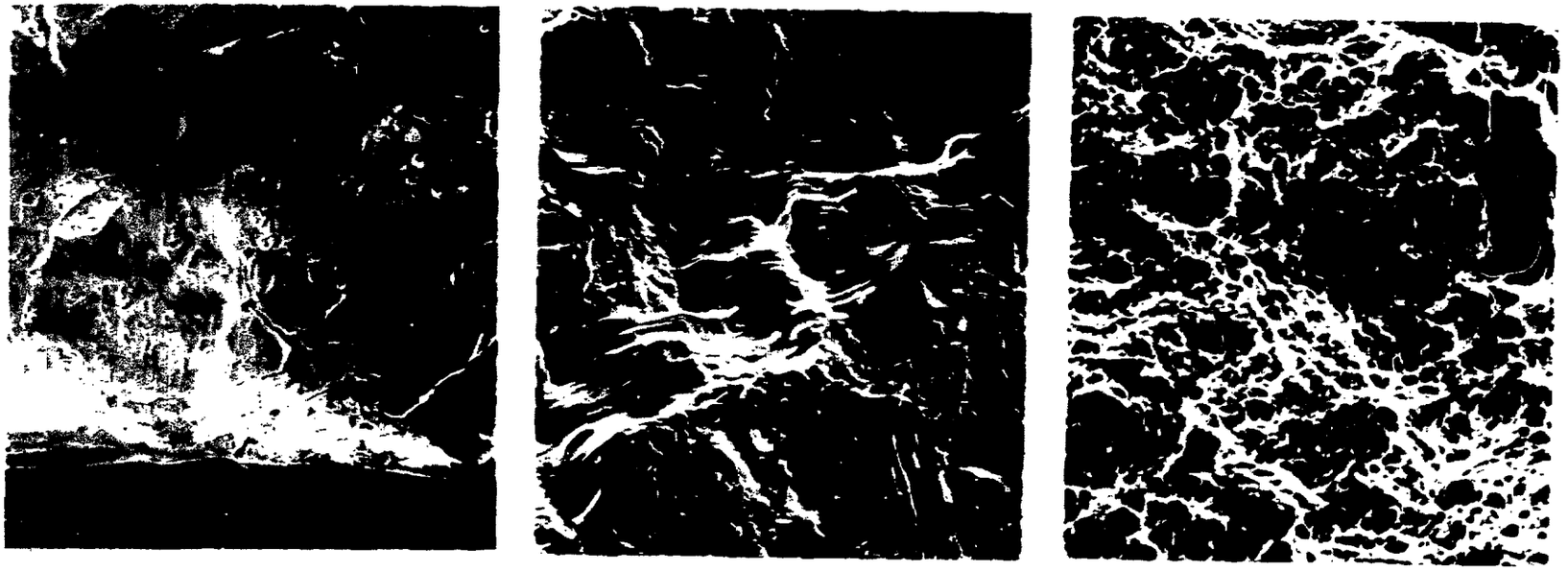

(a) Stress Corrosion Cracking at Rifling Land, 400X.

(b) Fatigue Cracking at Location 1 in Figure 9, 100X.

(c) Fast Fracture at Location 2 in Figure 9, 1700X.

Figure 10. Scanning Electron Microscope Fractographs of Stress Corrosion Initiated Cracking in a Cannon Tube.

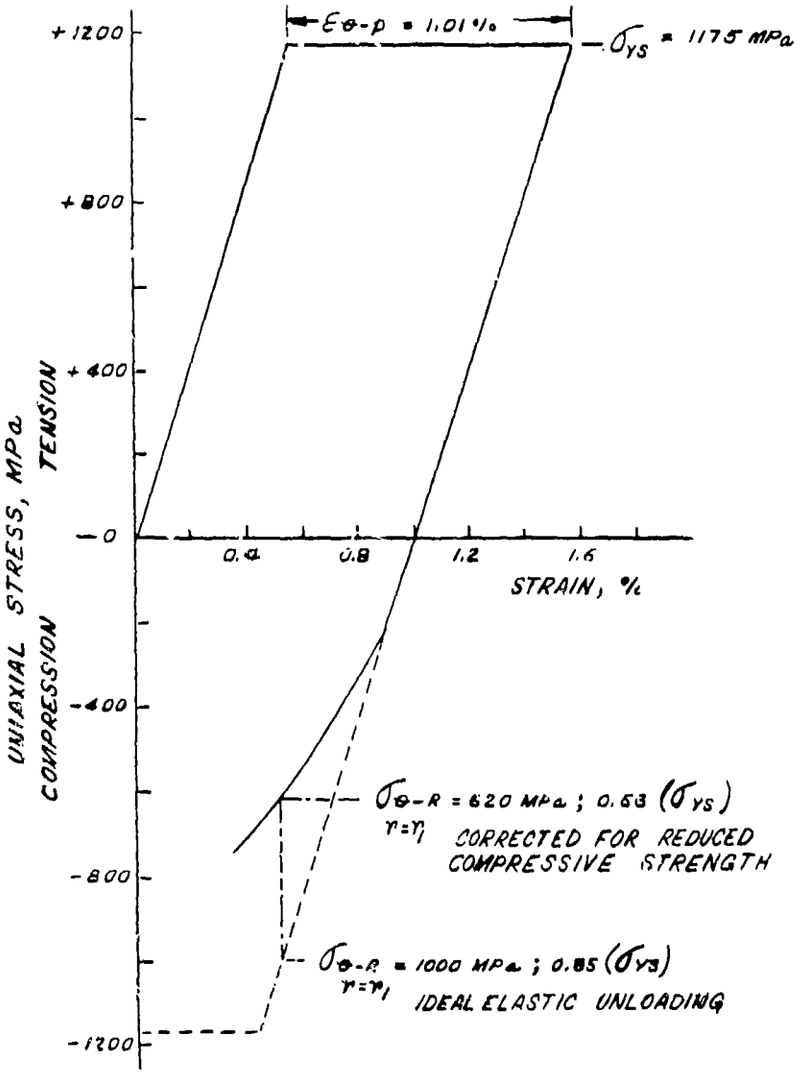

Figure 11. Sketch of Tensile Yielding and Reduced Compressive Yield Strength for 100% Overstrained Steel Cylinder with $r_2/r_1 = 2.0$.

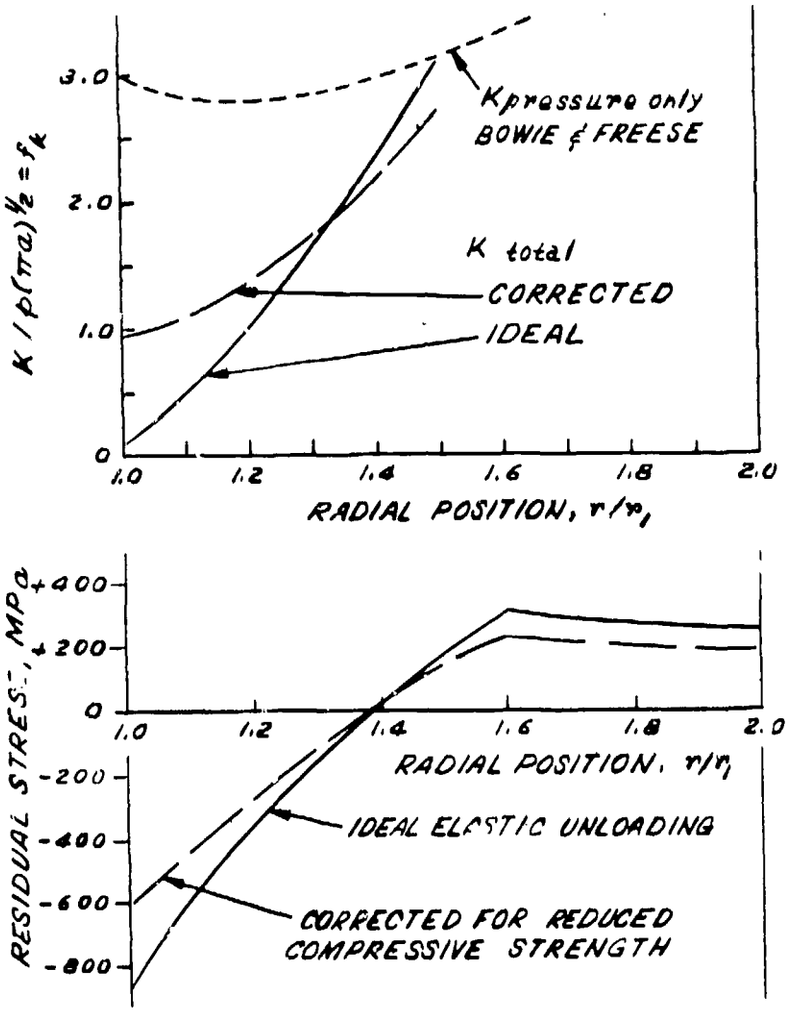

Figure 12. Residual Stress and Stress Intensity Factor, K, Distributions for 60% Overstrained Cylinder with r_1 = 2.0, p = 331 MPa, a_i = 6.4 mm, a/2c = 0.5.

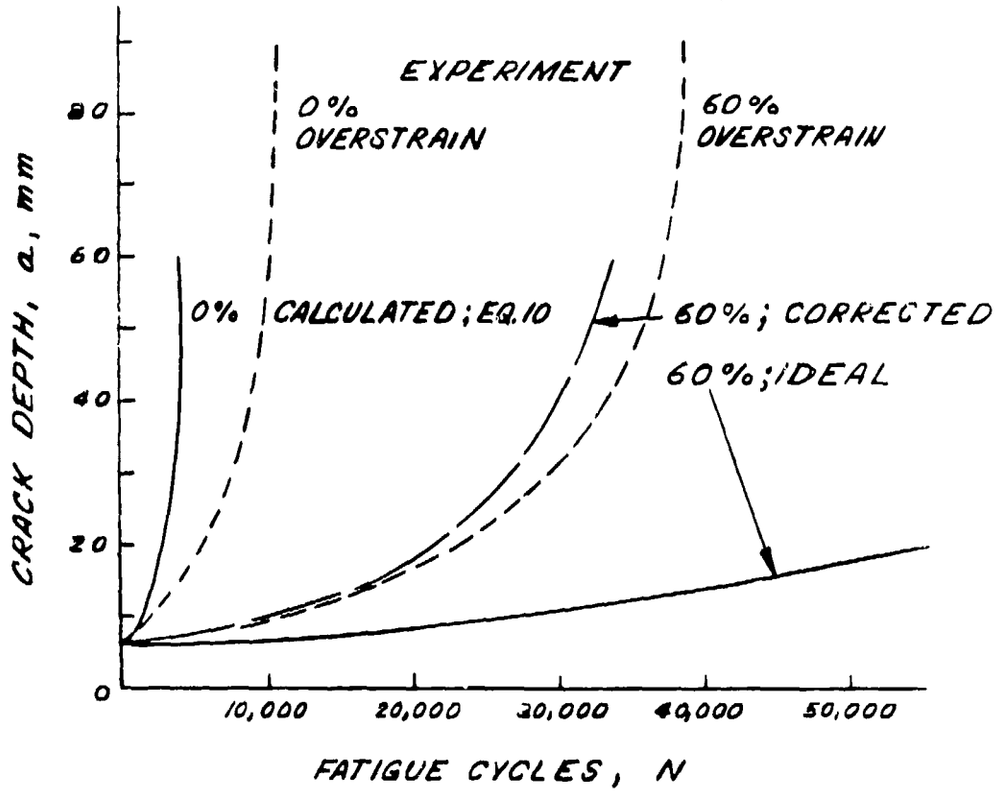

Figure 13. Crack Depth Versus Number of Fatigue Cycles From Experiment and Analysis for Cylinders with 0% and 60% Overstrain, r_1 = 90 mm, r_2/r_1 = 2.0, p = 331 MPa, a_i = 6.4 mm, a/2c = 0.5.

TECHNICAL REPORT INTERNAL DISTRIBUTION LIST

	NO. OF COPIES
COMMANDER	1
CHIEF, DEVELOPMENT ENGINEERING BRANCH	1
ATTN: DRDAR-LCB-DA	1
-DM	1
-DP	1
-DR	1
-DS (SYSTEMS)	1
-DS (ICAS GROUP)	1
-DC	1
CHIEF, ENGINEERING SUPPORT BRANCH	1
ATTN: DRDAR-LCB-SE	1
-SA	1
CHIEF, RESEARCH BRANCH	2
ATTN: DRDAR-LCB-RA	1
-RC	1
-RM	1
-RP	1
TECHNICAL LIBRARY ATTN: DRDAR-LCB-TL	5
TECHNICAL PUBLICATIONS & EDITING UNIT ATTN: DRDAR-LCB-TL	2
DIRECTOR, OPERATIONS DIRECTORATE	1
DIRECTOR, PROCUREMENT DIRECTORATE	1
DIRECTOR, PRODUCT ASSURANCE DIRECTORATE	1

NOTE: PLEASE NOTIFY DIRECTOR, BENET WEAPONS LABORATORY, ATTN: DRDAR-LCB-TL, OF ANY REQUIRED CHANGES.

TECHNICAL REPORT EXTERNAL DISTRIBUTION LIST

	NO. OF COPIES
ASST SEC OF THE ARMY RESEARCH & DEVELOPMENT ATTN: DEP FOR SCI & TECH THE PENTAGON WASHINGTON, D.C. 20315	1
COMMANDER US ARMY MAT DEV & READ. COMD ATTN: DRCDE 5001 EISENHOWER AVE ALEXANDRIA, VA 22333	1
COMMANDER US ARMY ARRADCOM ATTN: DRDAR-LC -LCA (PLASTICS TECH EVAL CEN) -LCE -LCM -LCS -LCW -TSS (STINFO) DOVER, NJ 07801	1 1 1 1 1 1 2
COMMANDER US ARMY ARRCOM ATTN: DRSAR-LEP-L ROCK ISLAND ARSENAL ROCK ISLAND, IL 61299	1
DIRECTOR US ARMY BALLISTIC RESEARCH LABORATORY ATTN: DRDAR-TSB-S (STINFO) ABERDEEN PROVING GROUND, MD 21005	1
COMMANDER US ARMY ELECTRONICS COMD ATTN: TECH LIB FT MONMOUTH, NJ 07703	1
COMMANDER US ARMY MOBILITY EQUIP R&D COMD ATTN: TECH LIB FT BELVOIR, VA 22060	1
COMMANDER US ARMY TANK-AUTMV R&D COMD ATTN: TECH LIB - DRDTA-UL MAT LAB - DRDTA-RK WARREN, MICHIGAN 48090	1 1
COMMANDER US MILITARY ACADEMY ATTN: CHMN, MECH ENGR DEPT WEST POINT, NY 10996	1
US ARMY MISSILE COMD REDSTONE SCIENTIFIC INFO CEN ATTN: DOCUMENTS SECT, BLDG 4484 REDSTONE ARSENAL, AL 35898	2
COMMANDER REDSTONE ARSENAL ATTN: DRSMI-RRS -RSM ALABAMA 35809	1 1
COMMANDER ROCK ISLAND ARSENAL ATTN: SARRI-ENM (MAT SCI DIV) ROCK ISLAND, IL 61299	1
COMMANDER HQ, US ARMY AVN SCH ATTN: OFC OF THE LIBRARIAN FT RUCKER, ALABAMA 36362	1
COMMANDER US ARMY FGN SCIENCE & TECH CEN ATTN: DRXST-SD 220 7TH STREET, N.E. CHARLOTTESVILLE, VA 22901	1
COMMANDER US ARMY MATERIALS & MECHANICS RESEARCH CENTER ATTN: TECH LIB - DRXMR-PL WATERTOWN, MASS 02172	2

NOTE: PLEASE NOTIFY COMMANDER, ARRADCOM, ATTN: BENET WEAPONS LABORATORY, DRDAR-LCB-TL, WATERVLIET ARSENAL, WATERVLIET, N.Y. 12189, OF ANY REQUIRED CHANGES.

TECHNICAL REPORT EXTERNAL DISTRIBUTION LIST (CONT.)

	NO. OF COPIES
COMMANDER US ARMY RESEARCH OFFICE P.O. BOX 12211 RESEARCH TRIANGLE PARK, NC 27709	1
COMMANDER US ARMY HARRY DIAMOND LAB ATTN: TECH LIB 2800 POWDER MILL ROAD ADELPHIA, MD 20783	1
DIRECTOR US ARMY INDUSTRIAL BASE ENG ACT ATTN: DRXPE-MT ROCK ISLAND, IL 61299	1
CHIEF, MATERIALS BRANCH US ARMY R&S GROUP, EUR BOX 65, FPO N.Y. 09510	1
COMMANDER NAVAL SURFACE WEAPONS CEN ATTN: CHIEF, MAT SCIENCE DIV DAHLGREN, VA 22448	1
DIRECTOR US NAVAL RESEARCH LAB ATTN: DIR, MECH DIV CODE 26-27 (DOC LIB) WASHINGTON, D.C. 20375	1 1
NASA SCIENTIFIC & TECH INFO FAC P.O. BOX 8757, ATTN: ACQ BR BALTIMORE/WASHINGTON INTL AIRPORT MARYLAND 21240	1

	NO. OF COPIES
COMMANDER DEFENSE TECHNICAL INFO CENTER ATTN: DTIA-TCA CAMERON STATION ALEXANDRIA, VA 22314	12 (2-LTD)
METALS & CERAMICS INFO CEN BATTELLE COLUMBUS LAB 505 KING AVE COLUMBUS, OHIO 43201	1
MECHANICAL PROPERTIES DATA CTR BATTELLE COLUMBUS LAB 505 KING AVE COLUMBUS, OHIO 43201	1
MATERIEL SYSTEMS ANALYSIS ACTV ATTN: DRXSY-MP ABERDEEN PROVING GROUND MARYLAND 21005	1

NOTE: PLEASE NOTIFY COMMANDER, ARRADCOM, ATTN: BENET WEAPONS LABORATORY, DRDAR-LCB-TL, WATERVLIET ARSENAL, WATERVLIET, N.Y. 12189, OF ANY REQUIRED CHANGES.